

Modeling of the propagation of atmospheric aerosols on small scales

M.S. Yudin and K. Wilderotter

*Institute of Computational Mathematics and Mathematical Geophysics,
Siberian Branch of the Russian Academy of Sciences, Novosibirsk, Russia
Universitet Bonn, Germany*

Received March 3, 1999

The development and application of two numerical models of aerosol transport under urban conditions are discussed. The microscale model is applied to buildings and city canyons of complicated shape using the finite-element method. The mesoscale model is based on finite differences and takes into account the structure of the Earth's surface with the help of the roughness length concept. The results of model calculations for different types of surface inhomogeneities are presented. Qualitative agreement between theory and measurement data is obtained.

1. Introduction

Detailed studies of aerosol propagation and associated climatic characteristics have attracted ever-growing interest.¹ Information about meteorological fields such as temperature, pressure, humidity, etc. is key to modeling transport and diffusion of aerosols. Such information is often obtained by using simplified engineering formulas for typical meteorological situations. However, in complicated regions, detailed mathematical models based on a detailed description of the corresponding physical processes are needed.²

To reduce the number of calculations, it is natural to calculate the meteorological background in two steps.³ The first step calculates the microclimate of the region in which the object of interest is located. In the second step the data obtained in the first step are used as input parameters in a detailed simulation of the meteorological and aerosol fields on a microscale. Correspondingly, in the present work we consider two types of models: mesoscale and microscale. The mesoscale model is based on the method of finite differences and used a "surface-tracking" coordinate system. The calculation region then becomes quite simple. However, the transformed equations become considerably more complicated for discretization. Generally speaking, such an approach is suitable only in the case of a fairly level surface.⁴ The microscale model is based on the method of finite elements and is applied for simulating processes in urban settings, where a smooth substitution of variables is no longer applicable.

The problem of simulating aerosol transport in the atmosphere has a number of characteristic features, including the necessity to construct economical algorithms that provide an adequate description of regions where the calculated fields vary abruptly without a significant refinement of the grid and suppress spurious oscillations near the aerosol-cloud propagation front. In Ref. 5 we considered a

variational approach to simulating transport and diffusion of aerosols. Here we use a simpler finite-element scheme based on the so-called Petrov–Galerkin approach, which consists in adding an artificial viscosity in the direction of the flux.⁶ This scheme possesses high accuracy and reliability.

Section 2 considers simulation of the meteorological fields based on the complete (non-hydrostatic) system of equations of atmospheric dynamics. The fields so obtained are used as a background against which the aerosol propagates. Section 3 addresses transport of a pollutant in the atmosphere for large Reynolds numbers, and the calculational algorithm used here is based on the Petrov–Galerkin method. Finally, Section 4 presents results of some preliminary numerical experiments, both for a simple region and for the case of orography with large spatial gradients. With the intention of using the considered models to simulate aerosol transport in urban settings, Section 4 also presents a sample calculation of atmospheric characteristics above a region of enhanced roughness.

2. Calculation of the meteorological background

The mesoscale (outer) model is based on the complete (non-hydrostatic) system of equations of atmospheric dynamics

$$\frac{dU}{dt} + \frac{\partial P}{\partial x} + \frac{\partial(G^{13}P)}{\partial \eta} = f_1(V - V_g) - f_2W + R_u,$$

$$\frac{dV}{dt} + \frac{\partial P}{\partial y} + \frac{\partial(G^{23}P)}{\partial \eta} = f_1(U - U_g) + R_v,$$

$$\frac{dW}{dt} + \frac{1}{G^{1/2}} \frac{\partial P}{\partial \eta} + \frac{gP}{C_s^2} = f_2U + g \frac{G^{1/2} \bar{\rho} \theta'}{\bar{\theta}} + R_w,$$

$$\frac{d\theta}{dt} = R_\theta, \quad \frac{ds}{dt} = R_s,$$

$$\begin{aligned} \frac{1}{C_s^2} \frac{\partial P}{\partial t} + \frac{\partial U}{\partial x} + \frac{\partial V}{\partial y} + \frac{\partial}{\partial \eta} \left(G^{13} U + G^{23} V + \frac{1}{G^{1/2}} W \right) = \\ = \frac{\partial}{\partial t} \left(\frac{G^{1/2} \bar{\rho} \theta'}{\theta} \right). \end{aligned}$$

The mesoscale model is discretized by finite differences and uses the following substitution of variables, which transforms a region with complicated orography into a region with simple structure:

$$\eta = H(z - z_s) / (H - z_s),$$

z_s is the height of the orography, H is the height of the simulation region. Here $H = \text{const}$.

$$G^{1/2} = 1 - z_s/H, \quad G^{13} = \frac{1}{G^{1/2}} \left(\frac{\eta}{H} - 1 \right) \frac{\partial z_s}{\partial x},$$

$$G^{23} = \frac{1}{G^{1/2}} \left(\frac{\eta}{H} - 1 \right) \frac{\partial z_s}{\partial y}.$$

The microscale (inner) model is discretized by finite elements and does not use the above substitution of variables.

In the equations $U = \bar{\rho}u$, $V = \bar{\rho}v$, $W = \bar{\rho}w$, $P = p'$, where p' , θ' are the deviations from the reference state of the pressure \bar{p} and potential temperature $\bar{\theta}$; s is the specific humidity, C_s is the speed of a sound wave, u_g and v_g are the components of the geostrophic wind, representing the synoptic part of the pressure, f_1 and f_2 are the Coriolis parameters, and g is the acceleration due to gravity.

The terms R_u , R_v , R_ω , R_θ , R_s describe processes on a subgrid scale. To parametrize the turbulence, we use a simple scheme based on the calculation of the Blakadar mixing path.² The ordinary logarithmic wind profiles between the surface and the first atmospheric layer are estimated. As the standard roughness we choose 0.1 m. The mesoscale model considers urban settings as regions of enhanced roughness (see the sample calculation in Section 4).

We will not dwell here on details of the formulation and numerical realization of the equations of atmospheric dynamics (see Refs. 5 and 6). We go on now to the algorithm of aerosol propagation.

3. Modeling of propagation of aerosols

The convection–diffusion equation for transport of a substance in the atmosphere has the following form¹:

$$\frac{\partial \Phi}{\partial t} = \nabla (\mathbf{K} \nabla \Phi - \mathbf{v} \Phi) - \lambda \Phi + f. \quad (1)$$

Here $\Phi(\mathbf{x}, t)$ is the aerosol concentration, $\mathbf{K}(\mathbf{x}, t)$ is the dispersion tensor, $\mathbf{v}(\mathbf{x}, t)$ is the wind velocity, $\lambda(\mathbf{x}, t)$ describes the chemical reactions, $f(\mathbf{x}, t)$ is the source or sink term, and $\mathbf{x} \in \mathbf{R}^d$, $d = 1, 2, 3$.

We discretize this problem by the so-called standard Galerkin method, sometimes also called the

Bubnov–Galerkin method (see, e.g., Ref. 8). This method gives good numerical results for moderate Reynolds numbers. However, for large Reynolds numbers, i.e., for the case when advection strongly dominates diffusion, the results obtained by the standard Galerkin method are strongly oscillatory and bear little resemblance to the exact solution. One way of suppressing undesirable oscillations is the Petrov–Galerkin method. To simplify the notation, we describe this method in simplified form. We assume that the process of aerosol transport is stationary and that chemical reactions are absent. Moreover, we assume that $\mathbf{K} = \text{const}$, $\mathbf{K} \leq 1$, and that the velocity vector \mathbf{v} is constant and normalized, i.e., $|\mathbf{v}| = 1$. We emphasize, however, that the following analysis can be easily generalized to the general case.

We denote as $\nabla_{\mathbf{v}} \Phi = v_x \frac{\partial \Phi}{\partial x} + v_y \frac{\partial \Phi}{\partial y} + v_z \frac{\partial \Phi}{\partial z}$ the derivative in the direction \mathbf{v} . Let the boundary of the region Γ consists of four parts $\Gamma_1, \Gamma_2, \Gamma_3, \Gamma_4$ (see the sample calculation in Section 4 below). Thus our problem takes the form

$$\begin{aligned} -K \Delta \Phi + \nabla_{\mathbf{v}} \Phi &= f, \\ \Phi &= \Phi^D \quad \text{on } \Gamma_2, \\ \frac{\partial \Phi}{\partial n} &= 0 \quad \text{on } \Gamma_1, \Gamma_3, \Gamma_4. \end{aligned} \quad (2)$$

We use the standard notation for the scalar product

$$(\Phi, \Psi) = \int_{\Omega} \Phi \Psi \, d\Omega, \quad (\nabla \Phi, \nabla \Psi) = \int_{\Omega} \nabla \Phi \nabla \Psi \, d\Omega.$$

Multiplying this equation by the test function $\Psi + \delta \nabla_{\mathbf{v}} \Psi$, where $\Psi = 0$, on Γ_2 , and integrating over Ω , we obtain

$$\begin{aligned} K(\nabla \Phi, \nabla \Psi) - K \delta (\Delta \Phi, \nabla_{\mathbf{v}} \Psi) + (\nabla_{\mathbf{v}} \Phi, \Psi + \delta \nabla_{\mathbf{v}} \Psi) = \\ = (f, \Psi + \delta \nabla_{\mathbf{v}} \Psi), \end{aligned} \quad (3)$$

where the term $K(\Delta \Phi, \Psi)$ was integrated by parts, and δ is a positive parameter which will be determined below. To formulate the discrete analog of this equation, we replace, in analogy with the standard Galerkin method, Φ and Ψ by the piecewise linear approximations $\bar{\Phi}$ and $\bar{\Psi}$, which interpolate exactly at the triangulation nodes.

Since the function $\bar{\Phi}$ is piecewise linear, $\Delta \bar{\Phi} = 0$ inside each triangle Ω_e and therefore $(\Delta \bar{\Phi}, \nabla_{\mathbf{v}} \bar{\Psi}) = 0$. Omitting the overplaced bar for convenience, Eq. (3) reduces to the form

$$\begin{aligned} K(\nabla \Phi, \nabla \Psi) + \delta (\nabla_{\mathbf{v}} \Phi, \nabla_{\mathbf{v}} \Psi) + (\nabla_{\mathbf{v}} \Phi, \Psi) = \\ = (f, \Psi + \delta \nabla_{\mathbf{v}} \Psi). \end{aligned} \quad (4)$$

The difference from the standard Galerkin form consists in the presence of the terms $\delta (\nabla_{\mathbf{v}} \Phi, \nabla_{\mathbf{v}} \Psi)$ and

$\delta(f, \nabla_v \Psi)$. Integrating the term $\delta(\nabla_v \Phi, \nabla_v \Psi)$ formally by parts, we obtain $-\delta(\nabla_{vv} \Phi, \Psi)$ ($\nabla_{vv} \Phi$ denotes the second derivative of Φ in the direction v). This means that it is possible to interpret the Petrov–Galerkin method as the addition of an artificial viscosity of magnitude δ in the direction v . The term $\delta(\nabla_v \Phi, \nabla_v \Psi)$ is also numerically discretized in an analogous way as the diffusion term in the standard Galerkin method. The remaining calculations were performed in the same way as in the standard Galerkin method.

Finally, the magnitude of the parameter δ is assigned to be $\delta = 0(h/\nabla)$, where h is a typical grid-cell size. Numerical experiments showed that values $\delta = ch/v$, where $0.2 \leq c \leq 1.5$, give completely satisfactory results.

In closing, we underscore the main difference between the Petrov–Galerkin method and the standard Galerkin method. The Petrov–Galerkin method is based on multiplying by a test function of the form $\Psi + \delta \nabla_v \Psi$, where Ψ is piecewise linear and continuous. In particular, the test functions are discontinuous due to the discontinuity of the term $\delta \nabla_v \Psi$. This means that the test functions belong to a space which differs from the space of test functions where the discrete solution Φ is sought. On the other hand, in the standard Galerkin method the spaces of simple functions and test functions coincide.

4. Sample calculations

Our first numerical experiments were performed for a regular region and their goal consisted in demonstrating the advantages of the Petrov–Galerkin method.

Consider the problem

$$-K\Delta\Phi + v_x \frac{\partial\Phi}{\partial x} + v_y \frac{\partial\Phi}{\partial y} = 0, \quad \Phi = \Phi^D \quad \text{on } \Gamma_2,$$

$$\Phi = 0 \quad \text{on } \Gamma_1, \Gamma_4, \quad \frac{\partial\Phi}{\partial n} = 0 \quad \text{on } \Gamma_3,$$

where $K = 10^{-3}$; $\mathbf{v} = (v_x, v_y) = (\cos 10^\circ, \sin 10^\circ)$; $\Omega = \{(x, y): 0 < x, y < 1\}$ is the unit square, and $\Gamma_1, \Gamma_2, \Gamma_3, \Gamma_4$ are the bottom, left boundary, top, and right boundary of Ω , respectively. Further, $\Phi^D = 0$ for $x = 0, 0 < y < 1/2$; $\Phi^D = 1$ for $x = 0, 1/2 < y < 1$. The finite-element grid consists of 512 triangular elements and is uniform along both the horizontal and the vertical.

The exact solution possesses both an inner layer and a boundary layer on Γ_4 . It turns out that the goodness of the numerical solution depends substantially on the choice of the parameter δ . Figure 1 is for $\delta = 1$. The calculations show that the solution becomes smoother if we introduce a larger artificial viscosity coefficient, but in the case of too large a viscosity the solution loses its information content.

The mesoscale model treats urban settings as regions of enhanced roughness. Let us consider the results of a simulation of a typical situation.

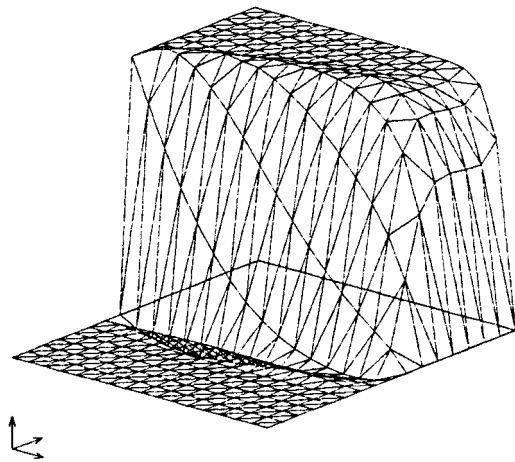


Fig. 1. Aerosol concentration in the Petrov–Galerkin method.

An island of 1-meter roughness is in the center of a region with dimensions 10 km × 10 km. The top of the calculation region is 5 km. A geostrophic flow propagates from west to east with a velocity of 5 m/s. As the reference state we adopt the standard atmospheric stratification with a gradient of 3.5 K/km. An absorbing layer is located above 1500 m. The calculational grid consists of 31 × 31 × 16 points with horizontal grid-cell size 333 m and variable vertical grid-cell size. Figure 2 shows a west-to-east cross section of the vertical velocity field through the center of the island. A relatively flat layer of uplift is seen above the region of roughness. The picture of the flow is found to be in qualitative agreement with theoretical predictions.⁹

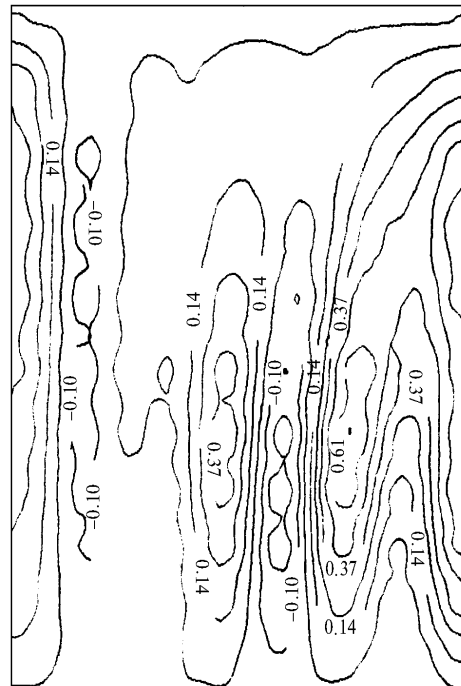


Fig. 2. Vertical velocity for enhanced roughness.

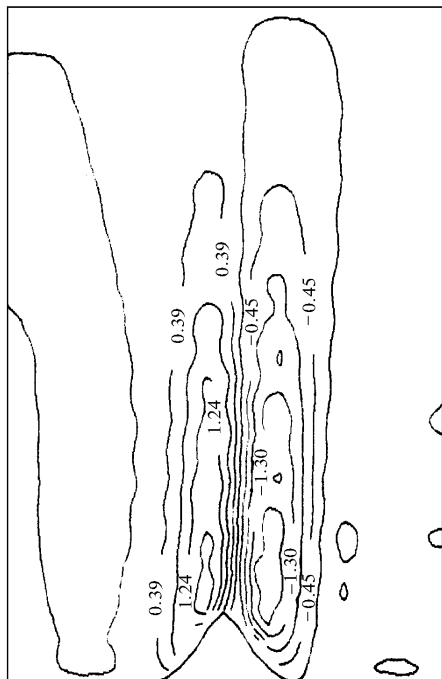


Fig. 3. Vertical velocity for enhanced orography.

We also performed an experiment with the inner model. Figure 3 shows the vertical velocity field for steady-state flow above an obstacle of the form $h = h_0 / (1 + x^2/a^2)$. Here $h_0 = 500$ m and $a = 500$ m. The dimensions of the region are $7 \text{ km} \times 5 \text{ km}$, the velocity of the outer flow is $u_g = 5 \text{ m/s}$, $v_g = 0$, and the 31×16 grid

consists of quadrilateral finite elements, which are uniform along the horizontal and become more densely distributed toward the surface. In the upper part of the region we have introduced a damping layer to decrease reflection of waves from the upper boundary. The stratification of the reference state is described by the standard atmosphere with a gradient of 3.5 K/km .

The overall structure of the flow corresponds to the available data.¹⁰

References

1. G.I. Marchuk, *Mathematical Modeling in Problems of the Environment* (Nauka, Moscow, 1982), 319 pp.
2. V.V. Penenko and A.E. Aloyan, *Models and Methods for Problems of Conservation of the Environment* (Nauka, Moscow, 1985), 256 pp.
3. J. Eichhorn, R. Schrodin, and W. Zdunkowski, *Beitr. Phys. Atmos.* **61**, No. 3, 187–203 (1988).
4. T. Clark, *J. Comp. Phys.* **24**, 186–215 (1977).
5. M.S. Yudin and K. Wilderotter, *Atmos. Oceanic Opt.* **11**, No. 10, 973–976 (1998).
6. M.S. Yudin, *Bull. Nov. Comp. Center, Num. Modeling Atmos.* **2**, 101–107 (1995).
7. A. Brooks and T. Hughes, *Comput. Meth. Appl. Mech. Eng.* **32**, 199–259 (1982).
8. G.I. Marchuk, *Methods of Computational Mathematics* (Nauka, Moscow, 1977), 316 pp.
9. R.D. Bornstein, *J. Appl. Meteorol.* **14**, 1459–1476 (1975).
10. T. Clark and R. Gall, *Mon. Weather Rev.* **110**, No. 7, 766–791 (1982).